Fano-type interference processes in linear photoluminescence spectra of infrared-driven quantum wells

1997 J. Phys.: Condens. Matter 9 7685

(http://iopscience.iop.org/0953-8984/9/36/016)

J. Phys.: Condens. Matter **9** (1997) 7685–7698. Printed in the UK PII: S0953-8984(97)79874-6

Fano-type interference processes in linear photoluminescence spectra of infrared-driven quantum wells

S M Sadeghi and J Meyer

The University of British Columbia, Department of Physics and Astronomy, 6224 Agricultural Road, Vancouver, BC, Canada V6T 1Z1

Received 27 November 1996, in final form 30 June 1997

Abstract. Quantum interference processes are investigated in the diagonal and nondiagonal excitonic emission spectra of quantum well structures coupled by single infrared fields polarized along their growth directions and resonant with the first-to-second-conduction-subband transitions. This investigation predicts generation of the Autler–Townes doublet in the emission spectrum of the coupled ground exciton state (diagonal transition) and development of a dynamic emission hole followed by a dark line in that of the higher coupled exciton states (nondiagonal transition). The characteristic limits determining these processes are determined and reported experimental results are explained successfully.

1. Introduction

An issue which is of great importance for both fundamental physical aspects and practical applications is the alteration of the photoluminescence (PL) spectrum of a quantum well (QW) in frequency and/or intensity. This can be achieved by applying an electric field to the QW [1], or by enhancing or inhibiting the spontaneous emission of QWs using optical microcavities [2]. The third method to change the PL spectrum of undoped QWs is to use optical fields. This process depends strongly on the polarization of the optical field. For intense far-infrared fields polarized in the QW plane the effect has been found to be quenching of the PL spectra [3]. If the optical field becomes polarized along the QW growth direction, however, the effect can be different in nature. Since in this case the conduction subbands of the QW can be mixed strongly by the infrared (IR) field, it can cause coherent mixing of the excitonic states associated with electrons in these subbands and holes in the valence band.

Investigation of this case, which based on our knowledge has not been studied in the past, is the subject of the present paper. We study here theoretically the quantum interference effects in the PL spectra of QWs coherently coupled by single IR fields. The optical field is polarized along the growth direction of the QW and resonant with the first- (E1-) to-second- (E2-) conduction-subband transition. Since the pumping process of the conduction subband is assumed to be the result of weak interband transitions, the coupling process is that between the corresponding exciton states (E1–HH1 and E2–HH1, see figure 1) due to strong correlation of the electrons in E1 and E2 and holes in HH1 (first hole subband). We show that while the ground coupled exciton emission can develop an Autler–Townes doublet, the higher coupled exciton decay can essentially undergo a different exotic development.

0953-8984/97/367685+14$19.50

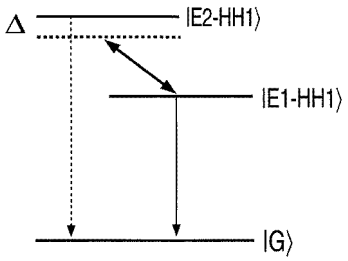

Figure 1. Excitonic coupling of a QW with an IR field. Δ refers to the detuning of the field, the solid downward arrow to the emission of the allowed transition, and the dashed downward arrow to that of the forbidden exciton. $|G\rangle$ is the ground state of the QW.

These developments include various quantum interference processes such as generation of an 'emission hole' in the decay spectrum followed by creation of a dark line [4]. We describe these evolutions as the result of Fano-type quantum interference processes caused by the infrared field and interband emission field. Also we discuss the characteristic limits which govern these phenomena and find out the role played by the damping rates of the excitons.

In order to study the PL spectra of IR-coupled QWs we have to consider two fields, one an interband (pump) field which generates electron–hole pairs, and the other an intersubband resonant (or near-resonant) IR field which mixes the exciton states. In section 2 the equations of motion of such a system are obtained [5]. The linear PL spectrum of this system is obtained in section 3 by the use of the linear response theory and the quantum regression theorem. In section 4 the results are applied to typical QW structures which present various physical systems. In section 5 we discuss the characteristic limits determining the evolution of the ground and higher coupled exciton emission spectra. In section 6 the discussion of PL dynamics in terms of LICS is presented. Section 7 contains concluding remarks of the study.

2. Equations of motion [5]

In the absence of the IR and pump fields the Hamiltonian of a QW has the following form:

$$H = H_0 + V. \tag{1}$$

Here H_0 is the Hamiltonian of single electrons in the valence and conduction bands given by

$$H_0 = \sum_{n_c,\boldsymbol{k}} E^c(n_c,k)a^\dagger_{n_c,\boldsymbol{k}}a_{n_c,\boldsymbol{k}} + \sum_{n_v,\boldsymbol{k}} E^v(n_v,k)a^\dagger_{n_v,\boldsymbol{k}}a_{n_v,\boldsymbol{k}}. \tag{2}$$

Here $E^c(n_v,k)$ and $E^v(n_v,k)$ are the single electron energies belonging to the conduction and valence bands respectively with n_c and n_v being the conduction and valence subband indices. $\boldsymbol{k}$ is the in-plane component of the electron wave-vector and the operator $a^\dagger_{n_c,\boldsymbol{k}}$ creates an electron in a conduction subband which is specified by $\boldsymbol{k}$ and n_c, and $a_{n_c,\boldsymbol{k}}$ annihilates such an electron. The same is assumed for $a^\dagger_{n_v,\boldsymbol{k}}$ and $a_{n_v,\boldsymbol{k}}$ in the valence band. Also we assume that the conduction subbands have parabolic dispersion with the same effective masses in the plane of the QW.

V describes the Coulomb interaction between carriers which generally contains electron–electron, hole–hole and hole–electron interactions. In this study, however, we are interested

in the low-pump-field excitation limit (linear PL). Therefore, the electron–electron and hole–hole scattering processes in the conduction and valence subbands are ignored. We also consider narrow single QW structures (∼7 nm well width) where the hole subbands are far from each other. Therefore, as shown in [6] and [7] the Coulomb mixing effect between the holes can be ignored. For the same reason the Coulomb interaction between electrons in different conduction subbands is ignored. Within these approximations V takes the following form:

$$V = \sum_{n_v n_c \boldsymbol{k}\boldsymbol{k}'\boldsymbol{q}\neq\boldsymbol{0}} V_{n_c,n_v}(\boldsymbol{k}', \boldsymbol{q}) a^{\dagger}_{n_c,\boldsymbol{k}+\boldsymbol{q}} a^{\dagger}_{n_v,\boldsymbol{k}'-\boldsymbol{q}} a_{n_v,\boldsymbol{k}'} a_{n_c,\boldsymbol{k}}. \tag{3}$$

Since the linear PL spectrum of the uncoupled QW at low temperature (∼10 K) is dominated by the excitonic states generated by the holes and electrons respectively in the first valence ($n_v = 1$), $|1, \boldsymbol{k}\rangle$, and conduction ($n_c = 2$), $|2, \boldsymbol{k}\rangle$, subbands (E1–HH1 exciton), we consider in our model these two subbands and the second conduction subband ($n_c = 3$), $|3, \boldsymbol{k}\rangle$.

Now let us consider the interaction of this system with an IR field near resonance with $|2, \boldsymbol{k}\rangle$ to $|3, \boldsymbol{k}\rangle$ (or E1 to E2) transitions. Within the rotating-wave and dipole approximations the interaction Hamiltonian involves the classical IR field, $E(t) = E\,\mathrm{e}^{\mathrm{i}\omega t}$, and is given by

$$H_1 = -\sum_{\boldsymbol{k}} \left\{ \mu_{23} E(t) a^{\dagger}_{3,\boldsymbol{k}} a_{2,\boldsymbol{k}} + \mu^{*}_{23} E^{*}(t) a^{\dagger}_{2,\boldsymbol{k}} a_{3,\boldsymbol{k}} \right\}. \tag{4}$$

Here μ_{23} is the electric dipole matrix element of transitions between the conduction subbands which is assumed to be $\boldsymbol{k}$-independent. Related to this equation one should note that in general an IR field causes transitions between eigenstates of the QW Hamiltonian (1) or the excitonic states. Using the assumption of equal transition dipole moments between excitonic states and between the conduction subbands [8] (4) can, however, represent the correct form of the coupling term.

To obtain the time evolution of the system we use the following equation for the density matrix of the system:

$$\frac{\partial \rho}{\partial t} = -\frac{\mathrm{i}}{\hbar}\big[H + H_1,\ \rho\big]. \tag{5}$$

After performing some algebra, for each set of three-subband states at a given $\boldsymbol{k}$ the equations of motion for each component of the density matrix of the IR-coupled QW in the presence of a pump field are obtained as follows:

$$\frac{\mathrm{d}}{\mathrm{d}t}\rho^{\boldsymbol{k}}_{11} = -\Gamma_1\left(\rho^{\boldsymbol{k}}_{11} - 1\right) + \Gamma^{r}_{21}\left(1 - \rho^{\boldsymbol{k}}_{11}\right)\rho^{\boldsymbol{k}}_{22} + \Gamma^{r}_{31}\left(1 - \rho^{\boldsymbol{k}}_{11}\right)\rho^{\boldsymbol{k}}_{33} + \lambda_1(\boldsymbol{k}) \tag{6}$$

$$\frac{\mathrm{d}}{\mathrm{d}t}\rho^{\boldsymbol{k}}_{22} = -\mathrm{i}\Omega\left(\rho^{\boldsymbol{k}}_{32} - \rho^{\boldsymbol{k}}_{23}\right) - \Gamma^{nr}_{2}\rho^{\boldsymbol{k}}_{22} - \Gamma^{r}_{21}\left(1 - \rho^{\boldsymbol{k}}_{11}\right)\rho^{\boldsymbol{k}}_{22} + \lambda_2(\boldsymbol{k}) \tag{7}$$

$$\frac{\mathrm{d}}{\mathrm{d}t}\rho^{\boldsymbol{k}}_{33} = -\mathrm{i}\Omega\left(\rho^{\boldsymbol{k}}_{23} - \rho^{\boldsymbol{k}}_{32}\right) - \Gamma^{nr}_{3}\rho^{\boldsymbol{k}}_{33} - \Gamma^{r}_{31}\left(1 - \rho^{\boldsymbol{k}}_{11}\right)\rho^{\boldsymbol{k}}_{33} \tag{8}$$

$$\frac{\mathrm{d}}{\mathrm{d}t}\rho^{\boldsymbol{k}}_{31} = \big[\mathrm{i}\big[E^{c}(3,\ k) + E^{h}(1,\ k) - \hbar\omega\big] - \gamma_{31}\big]\rho^{\boldsymbol{k}}_{31} + \mathrm{i}\sum_{\boldsymbol{q}\neq\boldsymbol{0}} V_{31}(\boldsymbol{k},\ \boldsymbol{q})\rho^{\boldsymbol{k}+\boldsymbol{q}}_{31}\left(\rho^{\boldsymbol{k}}_{33} - \rho^{\boldsymbol{k}}_{11}\right) + \mathrm{i}\Omega\rho^{\boldsymbol{k}}_{21} \tag{9}$$

$$\frac{\mathrm{d}}{\mathrm{d}t}\rho^{\boldsymbol{k}}_{21} = \big[\mathrm{i}\big[E^{c}(2,\ k) + E^{h}(1,\ k)\big] - \gamma_{21}\big]\rho^{\boldsymbol{k}}_{21} + \mathrm{i}\sum_{\boldsymbol{q}\neq\boldsymbol{0}} V_{21}(\boldsymbol{k},\ \boldsymbol{q})\rho^{\boldsymbol{k}+\boldsymbol{q}}_{21}\left(\rho^{\boldsymbol{k}}_{22} - \rho^{\boldsymbol{k}}_{11}\right) + \mathrm{i}\Omega\rho^{\boldsymbol{k}}_{31} \tag{10}$$

$$\frac{\mathrm{d}}{\mathrm{d}t}\rho^{\boldsymbol{k}}_{23} = \big[-\mathrm{i}\big(E^{c}(3,\ k) - E^{c}(2,\ k) - \hbar\omega\big) - \gamma_{23}\big]\rho^{\boldsymbol{k}}_{23} + \mathrm{i}\Omega\left(\rho^{\boldsymbol{k}}_{33} - \rho^{\boldsymbol{k}}_{22}\right). \tag{11}$$

Here we have $\rho_{ij}^{\boldsymbol{k}} = \rho_{ji}^{\boldsymbol{k}*}$. $E^h(1, k)$ refers to the hole energy in the first hole subband (HH1) and ω to the frequency of the IR field. $\Omega = -\mu_{23}E/\hbar$ is the Rabi frequency. As mentioned before, since in this study the electron–electron and hole–hole scattering processes can be ignored, the exchange terms have insignificant effect [9]. Therefore we dropped them from these equations. Also one should note that since (9) and (11) contain the infrared field frequency, they do not have the standard forms obtained previously in the case of multi-subband optical Bloch equations in the absence of an IR field [10].

In (6) the pump rate $\lambda_1(\boldsymbol{k})$ is introduced to represent the rate at which the first valence subband is depopulated by an interband optical pump field. Also $\lambda_2(\boldsymbol{k})$ shows the rate at which the first conduction subband is populated by this field and by the intersubband and intrasubband transitions of other electrons in states with higher energies. The pump field is assumed to have photon energy larger than that of the band gap and generates carriers with kinetic energy less than that of LO phonons [11].

In order to consider damping in (6)–(11), various phenomenological scattering rates, Γ_i, and dephasing rates, γ_{ij}, are introduced. These rates are introduced for the sake of the generality of these equations. When we transfer these equations into the exciton bases, we attribute to them a new set of damping rates. Briefly, Γ_3^{nr} is the nonradiative scattering rate of electrons in $|3, \boldsymbol{k}\rangle$. This arises mainly from the intersubband LO phonon–electron scattering processes. Γ_{31}^{r} is the decay rate of electrons in this subband due to the radiative recombination with holes in HH1. We recall that such a transition is possible only in asymmetric QWs. Γ_2^{nr} and Γ_{21}^{r} are the first-conduction-subband ($|2, \boldsymbol{k}\rangle$) nonradiative and radiative scattering rates respectively. Since we assume that Γ_{21}^{r} (and Γ_{31}^{r}) is nonzero only when the system is in a bound state (band–band emission is ignored), we put $\rho_{11}^{\boldsymbol{k}} = 0$ in the corresponding radiative pumping and decay terms in (6)–(8). Γ_1 in (6) is the scattering rate of electrons (or holes) in the ground valence subband and is mainly due to electron–electron and electron–phonon scattering processes. The γ_{ij} represent the polarization dephasing rates.

As mentioned in the introduction the IR coupling of the QW occurs basically between E1–HH1 and E2–HH1 exciton states. One can show that these states should have the same total and orbital angular momenta [12]. Therefore in narrow QWs, since the interband E1–HH1 excitation selection rules only allow excitation of s states [13], the IR field mainly couples excitons with the same s-type hydrogenic quantum number (n = 1s, 2s, etc). We can use the sets of exciton states to transfer each element of the density matrix in k-space into an excitonic basis. To do this we use the excitonic wave-functions associated with n_v and n_c, ϕ_{n_c,n_v}^{n}, obtained from

$$\left[E^c(n_c, k) + E^h(n_v, k)\right]\phi_{n_c n_v}^{n}(\boldsymbol{k}) - \sum_{\boldsymbol{q}\neq\boldsymbol{0}} V_{n_c n_v}(q)\phi_{n_c n_v}^{n}(\boldsymbol{k}+\boldsymbol{q}) = E_n^{n_c}\phi_{n_c n_v}^{n}(\boldsymbol{k}). \tag{12}$$

Here $E_n^{n_c}$ are the n_c–HH1 exciton binding energies which for simplicity can be considered to be equal for $n_c = 2$ and 3 [14]. Using the $\{\phi_{n_c n_v}^{n}\}$, each $\rho_{n_c 1}^{\boldsymbol{k}}$ can be expanded as follows:

$$\rho_{n_c 1}^{\boldsymbol{k}} = \sum_{n} \rho_{n_c 1}^{n}\phi_{n_c 1}^{n}(\boldsymbol{k}) \tag{13}$$

where n runs over all discrete and continuous states of n_c–HH1. For the diagonal elements and (11) either of these sets can be used.

For the QW structures considered in this paper the bound exciton states have the dominant contribution in their linear PL spectra. The equations of motion transferred into excitonic bases for such states are obtained as follows:

$$\frac{\mathrm{d}\rho_{11}^{n}}{\mathrm{d}t} = \frac{1}{\tau_2^n}\rho_{22}^{n} + \frac{1}{\tau_3^n}\rho_{33}^{n} - \lambda_n \tag{14}$$

$$\frac{\mathrm{d}\rho_{22}^{n}}{\mathrm{d}t} = -\mathrm{i}\Omega\left(\rho_{32}^{n} - \rho_{23}^{n}\right) - \frac{1}{\tau_{2}^{n}}\rho_{22}^{n} + \lambda_{n}' \tag{15}$$

$$\frac{\mathrm{d}\rho_{33}^{n}}{\mathrm{d}t} = -\mathrm{i}\Omega\left(\rho_{23}^{n} - \rho_{32}^{n}\right) - \frac{1}{\tau_{3}^{n}}\rho_{33}^{n} - \frac{1}{\tau_{3}^{n\prime}}\rho_{33}^{n} \tag{16}$$

$$\frac{\mathrm{d}\rho_{21}^{n}}{\mathrm{d}t} = \left(\mathrm{i}E_{n}^{1} - \frac{1}{T_{12}^{n}}\right)\rho_{21}^{n} + \mathrm{i}\Omega\rho_{31}^{n} \tag{17}$$

$$\frac{\mathrm{d}\rho_{31}^{n}}{\mathrm{d}t} = \left[\mathrm{i}\left(E_{n}^{2} - \bar{h}\omega\right) - \frac{1}{T_{13}^{n}}\right]\rho_{31}^{n} + \mathrm{i}\Omega\rho_{21}^{n} \tag{18}$$

$$\frac{\mathrm{d}\rho_{23}^{n}}{\mathrm{d}t} = \left(-\mathrm{i}\Delta - \frac{1}{T_{23}^{n}}\right)\rho_{23}^{n} + \mathrm{i}\Omega\left(\rho_{33}^{n} - \rho_{22}^{n}\right). \tag{19}$$

Here Δ is the detuning of the IR field given by

$$\Delta = E^{c}(3,k) - E^{c}(2,k) - \bar{h}\omega.$$

With the assumption of $E_{n}^{2} \sim E_{n}^{1}$, Δ can also represent the IR detuning for transitions between the s states of E1–HH1 and E2–HH1. $\tau_{n_c}^{n}$ and $\tau_{n_c}^{n\,\prime}$ are the phenomenological radiative and nonradiative relaxation times of electrons in the nth exciton state, respectively. $T_{n_v n_c}^{n}$ and $T_{n_c n_c'}^{n}$ are the polarization dephasing times associated with the excitonic transitions with the corresponding indices. They include contributions of the quasi-elastic exciton–acoustic phonon and inelastic exciton–LO phonon scattering processes.

λ_{n}' and $-\lambda_{n}$ are the generation rates of the electrons and holes corresponding to the nth state of the E1–HH1 exciton. As in the case of $\lambda_{2}(\boldsymbol{k})$, λ_{n}' includes the contribution from the pump field (after undergoing various electron– and exciton–phonon scattering processes) and that of electrons which are relaxed down from the higher conduction subband via nonradiative decay of E2–HH1. In fact in terms of these dynamics we consider in steady state fashion two effective loops both consisting of bound radiative E1–HH1 exciton $\rightarrow$ bound E2–HH1 exciton $\rightarrow$ free electron–hole pairs $\rightarrow$ bound radiative E1–HH1 exciton. One of the loops has leakage due to the radiative decay of bound E1–HH1 excitons (single symmetric QW), and the other has an additional leakage due to the radiative decay of E2–HH1 excitons (single asymmetric QW). The effective loops are based on the assumption that both IR and pump fields have quasi-time-independent amplitudes.

(14)–(19) can be reduced to a linear matrix equation as follows:

$$\frac{\mathrm{d}\boldsymbol{\Phi}}{\mathrm{d}t} = \mathbf{L}\boldsymbol{\Phi} + \boldsymbol{K} \tag{20}$$

where $\boldsymbol{\Phi}$ is a nine-element vector, containing the density matrix elements in the exciton basis $\{\rho_{ij}^{n}\}$ and $\mathbf{L}$, a 9×9 matrix, and $\boldsymbol{K}$, a nine-element column, are their coefficients.

3. Linear photoluminescence of an infrared-coupled quantum well

Because of the lack of translational symmetry for excitons along the growth direction, the radiative decay of an IR-coupled QW can be described in terms of the system polarization. Such a decay, however, depends in general on the carrier–carrier and carrier–phonon scattering processes, QW layer roughness (interface fluctuation), and other effects. These effects give rise to various phenomena such as memory effect (non-Markoffian process), renormalization of the transition energy and the Rabi frequency. Inclusion of these effects in the fast nonsteady-state cases where a large number of carriers are excited is necessary [15]. In our case, however, we are looking for a linear PL spectrum of the QW in a steady state fashion at low interband excitation where the carrier–carrier scattering can be ignored.

This means that as mentioned before the exchange effects, electron–exciton interaction and lifetime broadening due to the distribution of electrons and holes can be ignored. In fact we are dealing here with the emission spectra of uncorrelated single excitons (intrinsic case). These excitons, however, are optically mixed to another set of excitons by an IR field.

Using these facts one can show that the linear PL spectrum due to the decay of the nth E1–HH1 and E2–HH1 bound excitonic states can be found in terms of the two-time correlations of the system polarization, $\langle p_n^-(t)p_n^+(t')\rangle$ in which $t > t'$ [16]. Here p_n^- and p_n^+ are the positive- and negative-frequency parts of the polarization associated with the nth states of these excitonic sets and defined by

$$p_n^+ = \mu_{E1-HH1}^n b_n a_{n,E1} + \overline{\mu}_{E2-HH1}^n b_n a_{n,E2} \tag{21}$$

and $p_n^- = (p_n^+)^*$. The b_n and $a_{n,E1}$ ($a_{n,E1}$) are annihilation operators of the hole and electron in the nth excitonic state of E1–HH1 (E2–HH1) respectively. μ_{E1-HH1}^n is the interband transition dipole moment of E1–HH1 excitons, and $\overline{\mu}_{E2-HH1}^n$ is that of the E2–HH1 excitons. The sign over the latter dipole moment represents the parity consideration. For a symmetric QW this dipole moment is zero due to forbidden interband transition between E2 and HH1. Using the properties of the Laplace transform, the linear PL spectrum of the IR-coupled QW can in general have the following form:

$$S(\omega_r) = \mathrm{Re}\sum_n f_n\langle \hat{p}_n^-(z,\ t')p_n^+(t')\rangle\big|_{z=\mathrm{i}\omega_r}. \tag{22}$$

Here $\hat{p}_n^-(z,t')$ refers to the Laplace transform of $p_n^-(t) = p_n^-(t'+\tau)$ with respect to $\tau = t-t'$ ($\tau > 0$) and ω_r is the spontaneously emitted radiation field frequency. f_n is a factor which represents the thermal distribution of the excitons in the nth state. Also since no coupling between the continuum of the E1–HH1 exciton and the bound state E2–HH1 is considered, no Fano resonance caused by the Coulomb interaction is generated.

To calculate the linear PL spectrum of the IR-coupled QW (22) we have to find the spectrum associated with each state ($\langle \hat{p}_n^-(z,t')p_n^+(t')\rangle$) and then sum over n. To do this we first calculate $\langle p_n^-(t)\rangle$ and then use the quantum regression theorem to obtain the two-time correlation functions [17]. We also consider the variation of the pump and IR field amplitudes to be slow compared to the dephasing times of excitons. Therefore one can treat the system as in steady state conditions. By imposing these conditions ($t,\ t' \to \infty$), we obtain the following expression for $\langle \hat{p}_n^-(z,t')p_n^+(t')\rangle$ at a given n:

$$\begin{aligned}\langle \hat{p}_n^-(z)p_n^+(\infty)\rangle = {} & |\mu_{E1-HH1}^n|^2\Big\{R_{83}(z)\Phi_2(\infty) + R_{87}(z)\Phi_6(\infty) + R_{88}(z)\Phi_1(\infty) \\ & + \sum_j \frac{1}{z}R_{8j}(z)\Phi_6(\infty)K_j\Big\} + |\overline{\mu}_{E2-HH1}^n|^2\Big\{R_{33}(z')\Phi_9(\infty) \\ & + R_{37}(z')\Phi_5(\infty) + R_{38}(z')\Phi_4(\infty) + \sum_j \frac{1}{z'}R_{3j}(z')\Phi_5(\infty)K_j\Big\}.\end{aligned} \tag{23}$$

Here $R_{ij}(z)$ are the elements of the following matrix:

$$\mathbf{R}(z) = (z\mathbf{I} - \mathbf{L})^{-1} \tag{24}$$

where $\mathbf{I}$ refers to the identity matrix. The same is true for $z' = z - \mathrm{i}\omega$ if we substitute z by z' in (24). Also because of the steady state condition (20) is solved as follows:

$$\Phi_i(\infty) = -\sum_j \left(\mathbf{L}^{-1}\right)_{ij} K_j. \tag{25}$$

This condition is related to the assumption that the pump and IR fields have long duration compared to typical dephasing times of the system. Typical experiments can be performed

within these conditions [18]. By substituting (23) into (22), we obtain a general expression for the linear PL spectrum of an IR-coupled QW.

4. Results

In this section we use the formalism developed in sections 2 and 3 to study the PL spectra of different IR-coupled QW structures. Due to the fact that oscillator strengths of the excited states of excitons are decreased by $(n-\frac{1}{2})^{-3}$ and because of low temperature and low interband excitation we only consider emission of 1s states [19] with binding energies equal to $\sim$10 meV. We also consider the structures to be inhomogeneously broadened. For this reason the homogeneous line width is considered to be 0.6 meV to include both acoustic phonon and layer interface fluctuation quasi-elastic scattering processes with bound excitons [20]. We also follow the standard method of dealing with such cases by considering the exciton emission spectrum as a convolution of a Gaussian line-shape with Lorentzian emission spectra with a width equal to 0.6 meV [19].

4.1. Symmetric single quantum well, diagonal E1–HH1 emission

In this subsection we study the PL spectrum of a symmetric single QW coupled by an IR field. Here the parities of the subbands are well defined, and, therefore, only the E1–HH1 exciton can decay radiatively ($1/\tau_3^n = 0$). We start our investigation with a $GaAs/Ga_{0.7}Al_{0.3}As$ QW structure having a width of the order of 7 nm. In such a structure the first and second bound conduction subbands are separated from each other by $\sim$123 meV, close to the CO_2 laser photon energies [21]. We consider $1/\tau_3^{n\prime} = 5$ ps^{-1} [22] and $\mu_{23} = e \times 1$ nm. Taking this value for the dipole moment, we estimate the IR intensity as $I = 0.24\ \Omega^2$ MW cm^{-2} (Ω in ps^{-1}). For this structure we consider the FWHM of the Gaussian line-shape to be 4 meV.

Figure 2 shows the way in which the linear PL spectrum changes when the IR field is resonant with E1–HH1 to E2–HH1 transitions. The initial effect of the IR field is seen to be a broadening of the PL line (dashed line). By further increasing the IR intensity the spectrum develops a doublet structure centred at the uncoupled central emission frequency (dotted line). The doubling becomes magnified by a further increase in the IR intensity (dashed–dotted line). When we detune the IR field by $\Delta = -5$ meV, the main effect is seen to be a blue shift of the radiation emission spectrum (see figure 3). If one continues to increase the field intensity another peak far to the red end of the spectrum starts to appear.

4.2. Asymmetric single quantum well, nondiagonal E2–HH1 emission

In this subsection we study the nondiagonal PL spectrum or up-conversion process in asymmetric QW structures. In such structures the interband transition of electrons in E2 to HH1 is to some extent possible ($1/\tau_3^n \neq 0$). Therefore, we expect to observe the radiative recombination of E2–HH1 excitons once the IR field is turned one. Here we apply our formalism to explain the experiment performed in [18] and discuss and predict more interesting phenomena which may occur.

To investigate the experiment we use the parameters suggested in [18] for the $GaAl/Al_{0.3}Ga_{0.7}As$ structure. This means that we consider the ratio of the emission oscillator strengths of E2–HH1 to E1–HH1 (f_2/f_1) to be equal to 0.024, and the IR field to be resonant with the transition between these two states. Also we consider $\tau_3^{n\prime} = 2.5$ ps, as obtained in [18], and the FWHM of the Gaussian function to be equal to 1.5 meV. The theory is applied

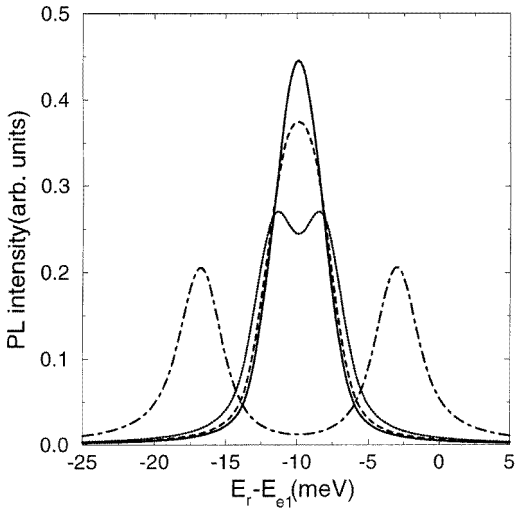

Figure 2. The 1s PL spectrum of the E1–HH1 exciton in the presence of a resonant IR field. The solid line corresponds to $\Omega = 0$, the dashed line to $\Omega = 1$ ps^{-1}, the dotted line to $\Omega = 2$ ps^{-1} and the dashed–dotted line to $\Omega = 10$ ps^{-1}. E_r and E_{e1} refer to energies of the emitted photons and that between the first conduction and valence subbands respectively. Here $1/T_{12} \sim 1$ ps^{-1} and $1/T_{13} \sim 6$ ps^{-1}.

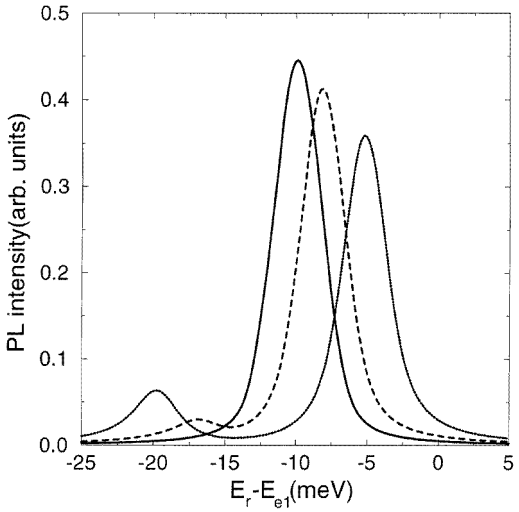

Figure 3. The 1s PL spectrum of the E1–HH1 exciton in the presence of a detuned infrared field, $\Delta = -5$ meV. The solid line corresponds to $\Omega = 0$, the dashed line to $\Omega = 5$ ps^{-1} and the dotted line to $\Omega = 10$ ps^{-1}. All other specifications are as for figure 2.

such that μ_{23} is considered to be a fitting parameter. Since the value of this parameter is well known, this approach has the benefit of testing the consistency of our theory with experiment. Consistent with our theory, the reference experiment has been performed at low temperature and the interband laser intensity was chosen to be low.

The results for the PL spectra of E2–HH1 are shown in figure 4. One can see that for

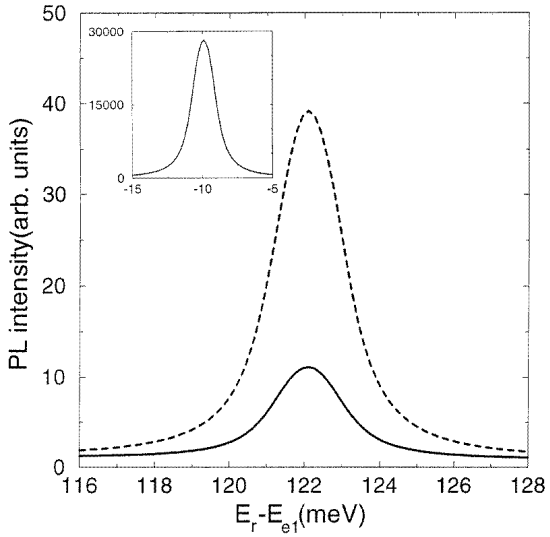

Figure 4. The nondiagonal exciton recombination of E2–HH1 in the presence of a resonant IR field. The solid line corresponds to emission at $\Omega = 0.08$ ps^{-1} and the dashed line to $\Omega = 0.16$ ps^{-1}. The inset shows the corresponding E1–HH1 emission. Here $1/T_{12} \sim 1$ ps^{-1} and $1/T_{13} \sim 1.5$ ps^{-1}.

$\Omega = 0$ ($I = 0$) there exists no emission from E2–HH1 exciton recombination (since no carrier exists in the second conduction subband), but when we increase the laser intensity to $\Omega = 0.08$ ps^{-1} (3.2 kW cm^{-2}) we see the generation of the up-conversion process (solid line). Further increase in the field intensity causes further increase in the intensity of such a process (see the dashed line for $I = 13$ kW cm^{-2} with $\Omega = 0.16$ ps^{-1}). The interesting result here resides in the ratio of the intensity of the E2–HH1 transition (I_2) to that of the E1–H1 transition (I_1) when they are simultaneously measured. Based on the experiment for an intensity of the IR field around $\sim$15 kW cm^{-2}, this ratio (I_2/I_1) should be $\sim$0.001. Using the inset of figure 4 which shows the intensity of E1–HH1 (I_1) simultaneous to the emission of E2–HH1, we find this ratio to be the same as that of the experiment. Such a consistency between the theory and experiment was found by putting $\mu_{23} = e \times 0.7$ nm ($I = 500\ \Omega^2$ kW cm^{-2}). One may find this value for the dipole moment a little small compared to those measured previously [23]. This can, however, be related to the relatively large value of the relaxation time found in [18] for the second conduction subband ($\tau_3^{n'} = 2.5$ ps). The value of μ_{23} would become larger if we considered a shorter relaxation time.

The results presented in figure 4 were limited to the intensities tested in the experiment. Now let us go forward and study the E2–HH1 radiation dynamics at higher IR intensities keeping other parameters the same as those of figure 4. One can see in figure 5 that increasing the field intensity causes further increase in the peak amplitude of the emitted light of E2–HH1 (solid line). However, a further increase in the IR intensity causes development of an 'emission hole' or dip at the line-centre frequency. This is accompanied by a further increase of the emission intensity (dashed line). Meanwhile the 'emission hole' becomes deeper while the emission peak amplitudes reach a saturated limit (dotted line). Finally when we apply high field intensities the 'emission hole' reaches a minimum and becomes virtually a dark line. At this condition further increase in the IR intensity causes further

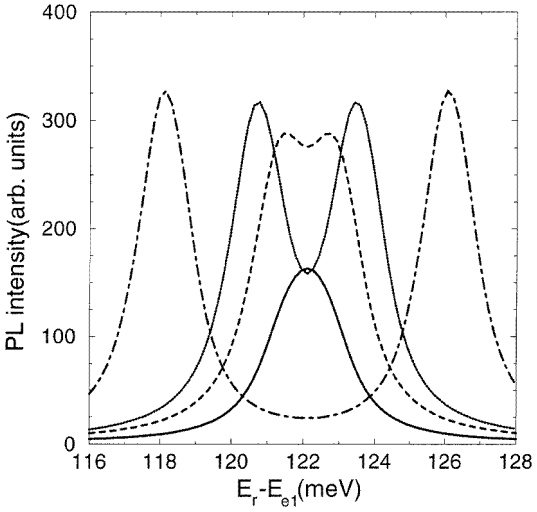

Figure 5. The nondiagonal exciton recombination of E2–HH1 in the presence of a resonant IR field. The solid line corresponds to emission at $\Omega = 0.4$ ps^{-1}, the dashed line to $\Omega = 1$ ps^{-1}, the dotted line to $\Omega = 2$ ps^{-1} and the dashed–dotted line to $\Omega = 6$ ps^{-1}. All other specifications are as for figure 4.

separation of the symmetric peaks of emission with no change in their shapes. The physical reasons for such phenomena will be discussed in sections 5 and 6.

5. Damping rate effects and characteristic limits

The evolutions of PL spectra studied in this paper present two different kinds of dynamic. The first type, which happens in both E1–HH1 and E2–HH1 exciton emissions, is a measure of the quantum interfering processes. They can be characterized in terms of the damping rates of the excitons and are scaled by the Rabi frequency. Based on our calculations this kind of dynamic falls into three characteristic limits. When we detect the E1–HH1 exciton emission these limits are (i) $\Omega \ll 1/T_{13}^n$ (the low-field limit) in which the coupling effect is seen as broadening of the E1–HH1 PL spectrum, (ii) $\Omega \sim 1/T_{13}^n$ where the spectrum starts to develop a doublet and (iii) $\Omega \gg 1/T_{13}^n$ or the high-field limit where the doublet becomes well resolved. Any further increase in the IR intensity beyond the high-field limit only causes more separation of the doublet peaks (see figure 2).

A similar dynamic can also be obtained in the evolution of E2–HH1 exciton decay, but such a dynamic is convoluted by a second type of dynamic caused by the rate at which E2–HH1 excitons are generated. Such a rate, which is only present in the E2–HH1 emission decay, depends on the damping rate of these excitons ($1/T_{13}^n$) and Ω. Therefore in contrast to the E1–HH1 emission, which was characterized by a single parameter ($1/T_{13}^n$), emission of E2–HH1 should be characterized by two parameters, $1/T_{12}^n$ and $1/T_{13}^n$. The former parameter provides the same information as $1/T_{13}^n$ did for E1–HH1. Considering figure 5 it gives the limits in which the E2–HH1 spectrum develops as a growing single peak ($\Omega \ll 1/T_{12}^n$, solid line), or starts to develop a dip or 'emission hole' ($\Omega \sim 1/T_{12}^n$, dashed line), or generates a well resolved doublet or dark line ($\Omega \gg 1/T_{12}^n$, dashed–dotted line). On the other hand, the amount of increase of the emission intensity of this state is characterized by $1/T_{13}^n$. If $\Omega \ll 1/T_{13}^n$ any increase of Ω generates a linear increase in the

E2–HH1 exciton emission, for $\Omega \sim 1/T_{13}^n$ this reaches a saturated limit and at the condition $\Omega \gg 1/T_{13}^n$ it becomes constant.

We also note that the relative magnitude of $1/T_{12}^n$ and $1/T_{13}^n$ is important in the evolution of the E1–HH1 and E2–HH1 emission spectra. In QWs, since $1/T_{13}^n > 1/T_{12}^n$ the basic development of the E1–HH1 emission should be mostly broadening, and the corresponding dynamics of the E2–HH1 emission should be the development of a single growing spectrum followed by an 'emission hole'. In other words, the conditions $\Omega < 1/T_{13}^n$ and $\Omega \sim 1/T_{12}^n$ are respectively likely regimes for the E1–HH1 and E2–HH1 evolution.

6. Fano-type quantum interference in the exciton emission spectra

Two interesting features seen in section 4 were the broadening followed by doubling of the E1–HH1 emission spectrum and generation of an emission hole followed by a dark line in that of E2–HH1. These features can be related to the dark-line effect and the Autler–Townes doublet previously discussed in atomic systems [24, 25]. It has been shown that in such systems, when the higher transition level of a two-level system was coupled by a laser field to a metastable state, its emission spectrum split into two parts with equal amplitudes as that of the uncoupled peak but of half the width. When the metastable state was substituted by a broad state the effect became broadening of the emission spectrum followed by the resolution of a doublet (Autler–Townes doublet) [25]. These processes have been interpreted in terms of quantum interferences between various transition paths of the system and the renormalization effects of the coupled state widths.

In this section we discuss the role played by quantum interferences in the emission of excitons in the IR-coupled QWs. However, instead of a mere interpretation we present a model which can visualize clearly the concept of quantum interferences in these systems and be used to describe the evolution of emission and absorption spectra of various systems in the low-field limit. The detailed quantitative features of this model have been presented in [25] for the case of an atomic system. Also its applications to explain conduction intersubband absorption dynamics of IR-coupled n-doped QWs at the low-field limit have been presented in [17] and [26]. This model is based on borrowing the laser-induced structure (LICS) concept from atomic physics. LICS can be obtained by embedding a bound state of an atom in the continuum using laser radiation. The shape of this induced structure, which may have asymmetric or symmetric profiles, is usually described by the Fano parameter, q [27]. When $q = 0$ we see a Lorentzian symmetric 'hole' driven into the (flat) continuum. For $|q| > 0$ we expect to see an asymmetric line-shape and in the limit of $|q| \gg 0$ a Lorentzian profile to develop.

Based on this model the emission dynamics of each discrete state of E2–HH1 can be considered as if it is structured by the optical embedding of a discrete E1–HH1 state into its line-centre vicinity, similar to LICS. In fact here the relatively narrow E1–HH1 acts as a bound state and the broad discrete state of E2–HH1 as an 'effective continuum'. To see this clearly we consider the evolution of nondiagonal emission of excitons considering two discrete E1–HH1 and E2–HH1 states with $1/T_{12} = 0.001$ ps^{-1} (unrealistic for quantum wells) and $1/T_{13}^n = 5$ ps^{-1}. This also has the benefit of showing the effects of damping rates and establishing a close correspondence to the ongoing discussion of quantum interference in atomic systems. The effects of actual damping rates of excitons enter as resolution parameters and cause line broadening in the results obtained at this limit of damping rates. Also the case of the inhomogeneous broadening effect can be obtained by speculating the results of the resonant and off-resonant coupling cases discussed in this section.

Under these conditions the results of detection of a single E2–HH1 discrete state PL

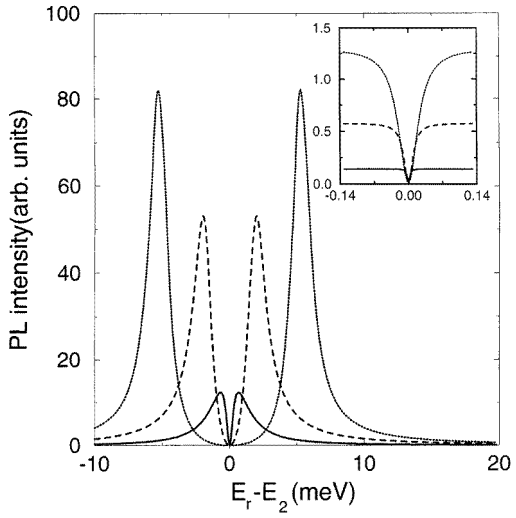

Figure 6. The nondiagonal exciton recombination of a discrete E2–HH1 exciton in the presence of a resonant IR field. The solid line corresponds to $\Omega = 1$, the dashed line to $\Omega = 3$ ps^{-1} and the dotted line to $\Omega = 8$ ps^{-1}. E_2 refers to the energy of the bound 1s E2–HH1 exciton and $1/T_{12} = 0.001$ ps^{-1} and $1/T_{13} = 5$ ps^{-1}. The inset shows similar a process at the earlier stage of coupling. The solid line here corresponds to $\Omega = 0.1$, the dashed line to $\Omega = 0.2$ ps^{-1} and the dotted line to $\Omega = 0.3$ ps^{-1}.

spectrum are shown in figure 6. Here we see that the PL spectrum from its early development has a dark line. This is because Ω reaches the limit of $\Omega \gg 1/T_{12}$ very early. Therefore, the phase of dynamic 'emission hole' is virtually skipped. Any increase in the field intensity makes the dark line wider and their corresponding peaks stronger and shifts them farther away from each other. Since at resonant coupling the photon energy of the laser is at the line peak of the E2–HH1 spectrum, the symmetry seen by the coupling field requires the induced structure to be the generation of a 'hole' within the 'effective continuum'. The inset of figure 6 shows this in more detail at the earlier stages of the coupling process at the vicinity of the line-centre frequency. In fact within the low-field limit any increase in the field intensity increases the magnitude of emission intensity while the dark line remains Lorentzian and becomes wider and deeper. This is a characteristic feature of a symmetrically structured state which is associated with LICS with $q = 0$. In fact at this limit the 'effective continuum' acts as the flat continuum of LICS [25, 27].

To describe the effect of detuned coupling we consider a case where $\Delta = +3$ meV. The result of the detection of the E2–HH1 PL spectrum with the same parameters as those in figure 6 is shown in figure 7. In contrast to figure 6, we see here the effect of the IR field as development of an asymmetric spectrum. For low IR intensities the spectrum includes an essential spectrum with a narrow structure at its tail (solid line). Increasing the IR intensity makes the essential peak and structure larger in amplitude and shifts them away from each other. This process is accompanied by narrowing the essential peak and broadening the structure until they become identical and Lorentzian at the high-field limit. In the inset of figure 7 we show the structured part of figure 7 at the early stage of its evolution. As one can see here the structure profiles at this range of the field intensity are similar to the standard Fano profiles seen in the discussion of LICS with $q \neq 0$ [27]. This requires an asymmetric coupling between these two states, as is the case since the IR field now sees

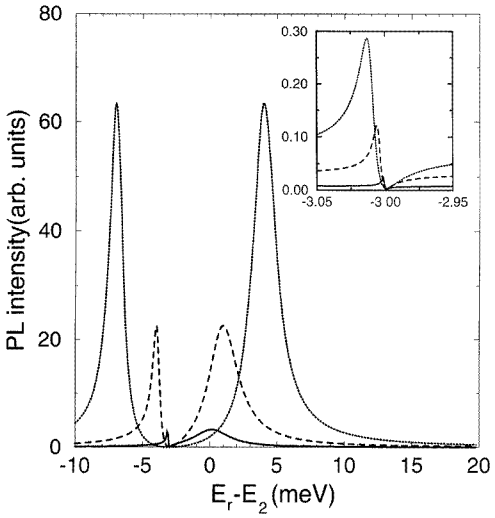

Figure 7. The 1s PL spectrum of a discrete E2–HH1 exciton in the presence of an IR field with $\Delta = +3$ meV. All other specifications are the same as for figure 6. The inset shows the structured parts of the emission spectra at the earlier stage of the coupling process. The solid line here corresponds to $\Omega = 0.1$, the dashed line to $\Omega = 0.2$ ps^{-1} and the dotted line to $\Omega = 0.3$ ps^{-1}.

the E2–HH1 spectrum asymmetrically. Increasing the IR intensity causes an increase in the amplitude of the structure emission accompanied by a definite amount of optical Stark shift. Such a shift can serve as a feature to establish a clearer relation between LICS and the discussed structuring process in this paper [25].

The picture presented in this section can be used to explain the physical processes beyond the results of numerical calculation. This can be done by inspecting the decay spectrum dynamics of the coupled pairs of exciton states. In fact they carry various Fano-type interferences characterized by their corresponding IR detunings. All of these spectra open a Fano-type window at the same frequency ($-\Delta$) due to destructive interference between the Raman paths which connect the ground state of the QW to the ground state of the E1–HH1 exciton through the middle state (E2–HH1), and the stepwise paths which connect the decaying E2–HH1 state to the ground state of the QW.

7. Conclusion

We studied the dynamics of the QW linear PL spectra in the presence of single IR fields. We showed that when such fields were polarized along the QW growth direction they can coherently change the PL spectrum of the ground state emission of the E1–HH1 exciton and that of the nondiagonal (forbidden) transitions such as the E2–HH1 exciton. The dynamics of the E1–HH1 emission spectra were shown to be broadening followed by doubling. The emission spectra of the E2–HH1 excitons (nondiagonal transitions) in asymmetric QWs were shown to be generation of a single growing emission peak followed by development of an 'emission hole' and dark line. These processes were shown to depend characteristically on the exciton dephasing rates. The emission spectra were analysed in terms of quantum interference between the Raman and stepwise paths analogous to the LICS. Using the concepts developed in this paper we also explained theoretically a recent

experiment involving the PL spectrum of an asymmetric QW in the presence of an IR field.

Acknowledgment

This research is supported by the Natural Science and Engineering Research Council of Canada.

References

[1] Polland H J, Schultheis L, Kuhl J, Gobel E O and Tu C W 1985 *Phys. Rev. Lett.* **55** 2610
[2] For a review see Yamamoto Y (ed) 1990 *Coherence, Amplification and Quantum Effects in Semiconductor Lasers* (New York: Wiley)
[3] Quinlan S M, Nikroo A, Sherwin M S, Sundaram M and Gossard A C 1992 *Phys. Rev.* B **45** 9428
[4] These are mostly atomic nomenclatures which refer to a relative decrease in the emission intensity (emission hole) or to nearly no intensity (dark line) at a specific frequency of the emission spectra.
[5] This section explains how one can derive the equations of motion from the very beginning in k-space. However, one can consider the main results of this section, (14)–(19), as a phenomenological model.
[6] Winkler R 1995 *Phys. Rev.* B **51** 14 395
[7] Zhu B and Huang K 1987 *Phys. Rev.* B **36** 8102
[8] For experiment see Li W J, McCombe B D, Chambers F A, Devane G P, Ralston J and Wicks G 1990 *Phys. Rev.* B **42** 11 953
[9] Binder R, Koch S W, Lindberg M, Schafer W and Jahnke F 1991 *Phys. Rev.* B **43** 6520
[10] Tsang L, Chansungsan and Chuang S L 1992 *Phys. Rev.* B **45** 11 918
[11] This assumption is applied for the sake of definiteness of the discussion. In practice the pump field can have a higher frequency. In this case the photo-excited carrier can have an initial fast scattering with LO phonons until they reach kinetic carrier lower than that of an LO phonon (see [18]).
[12] Sadeghi S M, Young J F and Meyer J 1996 unpublished
[13] Andreani L C and Pasquarello A 1990 *Phys. Rev.* B **42** 8928
[14] This assumption is basically supported by experiment (see [18]).
[15] Kuhn T and Rossi F 1992 *Phys. Rev.* B **46** 7496
[16] Mollow B R 1972 *Phys. Rev.* A **5** 2217
[17] Sadeghi S M, Young J F and Meyer J 1995 *Phys. Rev.* B **51** 13 349
[18] Vagos P, Boucaud P, Julien F H, Lourtioz J-M and Planel R 1993 *Phys. Rev. Lett.* **70** 1018
[19] Damen T C, Shah J, Oberli D Y, Chemla D S, Cunningham J E and Kuo J M 1990 *Phys. Rev.* B **42** 7434
[20] Citrin D S 1993 *Phys. Rev.* B **47** 3832
[21] Bastard G 1988 *Wave Mechanics Applied to Semiconductors Heterostructures* (Les Ulis: Editions de Physique)
[22] Ahn D and Chaung S L 1987 *J. Appl. Phys.* **62** 3052
[23] Capasso F, Sirtori C and Cho A Y 1994 *IEEE J. Quantum Electron.* **QE-30** 1313
[24] Zhu Shi-Yao, Narducci L M and Scully M O 1995 *Phys. Rev.* A **52** 4791
[25] Sadeghi S M and Meyer J to be published
[26] Sadeghi S M and Meyer J 1996 *Phys. Rev.* B **53** 10 094
[27] Cohen-Tannoudji C, Dupont-Roc J and Grynberg G 1992 *Atom–Photon Interactions* (New York: Wiley)